# Design of Circularly Symmetric Two-Dimensional Recursive Filters

JOSÉ M. COSTA, STUDENT MEMBER, IEEE, AND ANASTASIOS N. VENETSANOPOULOS, MEMBER, IEEE

*Abstract*—**The digital filtering of two-dimensional signals offers the many advantages characteristic of digital computers, such as flexibility and accuracy. Applications exist in the processing of images and geophysical data. A technique is presented for designing stable two-dimensional recursive filters whose magnitude response is approximately circularly symmetric. This is achieved by cascading a number of elementary filters which are called rotated filters because they are designed by rotating one-dimensional continuous filters and using the two-dimensional $z$-transform to obtain the corresponding digital filter. Stability of these filters is considered in detail and the results obtained are stated in two corollaries. In particular it is proved that rotated filters are stable if the angle of rotation is between 270° and 360°. Finally, methods of analysis and design of the shape, circular symmetry, and cutoff frequency of two-dimensional recursive filters are discussed.**

## I. INTRODUCTION

THE digital filtering of two-dimensional signals offers the many advantages characteristic of digital computers, such as flexibility and accuracy. Applications exist in the processing of images and geophysical data. In image processing there is no preferred spatial frequency axis. It is therefore desirable to process images with filters whose frequency response is approximately circularly symmetric.

The design techniques for nonrecursive filters in one dimension can often be extended to two dimensions in order to obtain filters with circularly-symmetric magnitude response [1]–[3]. On the other hand, the design of recursive filters in two dimensions becomes difficult due to the fact that a polynomial in two variables $P(z_1,z_2)$ cannot in general be factored into first- or second-order polynomials. This implies that many one-dimensional design techniques cannot be readily extended to two dimensions and that a high-order two-dimensional filter cannot in general be realized in parallel or cascade form to reduce the effect of quantization noise. It is also difficult to test the stability of two-dimensional recursive filters except for simple filters. Because of these difficulties, little work has been done on designing two-dimensional recursive filters, even though the use of recursive instead of nonrecursive filters has the potential of saving both computer time and computer memory [4]. A technique exists for mapping one-dimensional into two-dimensional filters with arbitrary directivity in a two-dimensional frequency response plane [5], [6]. These filters are called rotated filters because they are obtained by rotating one-dimensional filters.

In this paper we show how to cascade a number of rotated filters in order to obtain a stable circularly-symmetric filter. This approach approximates the circular-shaped contour levels of the magnitude response by a polygonal shape.

In Section II we review some concepts on two-dimensional recursive filters that will be used later in the paper. Section III shows a generalization of the technique of Shanks [6] to design rotated filters and in Section IV we solve the problem of determining the stability of rotated filters beforehand. The technique for designing circularly symmetric recursive filters is described in Section V. Finally, in Section VI we show briefly some methods of analysis and design of the shape, circular symmetry, and cutoff frequency of two-dimensional recursive filters.

Manuscript received December 28, 1973; revised May 29, 1974. This work was supported by the National Research Council of Canada under Grant No. A-7397.

The authors are with the Department of Electrical Engineering, University of Toronto, Toronto, Ont., Canada.

## II. TWO-DIMENSIONAL RECURSIVE FILTERS

A two-dimensional recursive filter can be described by a linear difference equation. The general form is

$$g(m,n) = \sum_{i=1}^{M_a} \sum_{j=1}^{N_a} a_{ij} f(m-i+1,n-j+1) - \sum_{i=1}^{M_b} \sum_{j=1}^{N_b} b_{ij} g(m-i+1,n-j+1), \quad (1)$$

$i,j \neq 1$ simultaneously.

Here it is assumed either that all output values $g(m-i+1,n-j+1)$ have been computed previously or are equal to zero (boundary conditions).

Equation (1) can be rewritten in the form

$$\sum_{i=1}^{M_b} \sum_{j=1}^{N_b} b_{ij} g(m-i+1,n-j+1) = \sum_{i=1}^{M_a} \sum_{j=1}^{N_a} a_{ij} f(m-i+1,n-j+1) \quad (2)$$

where $b_{11} = 1$.

Equation (2) can be solved for $g(m,n)$ [cf. (1)], $g(m-M_b+1,n)$, $g(m,n-N_b+1)$, or $g(m-M_b+1, n-N_b+1)$ and in each case the difference equation obtained corresponds to a two-dimensional recursive filter recursing in the $(+m,+n)$, $(-m,+n)$, $(+m,-n)$, or $(-m,-n)$ directions, respectively [7].

A recursive filter is said to be causal if it recurses in the $(+m,+n)$ direction [7]. A causal filter is realizable if its impulse response satisfies the property

$$h(m,n) = 0, \qquad m,n < 0.$$

A useful representation of (2) is obtained by the two-dimensional $z$ transform or double $z$ transform. This transform is defined as follows

$$X(z_1,z_2) \triangleq \sum_{m=-\infty}^{\infty} \sum_{n=-\infty}^{\infty} x(m,n) z_1^m z_2^n \tag{3}$$

where $x(m,n)$ is a two-dimensional sequence and $X(z_1,z_2)$ its two-dimensional $z$ transform.[1] The domain of definition for $X(z_1,z_2)$ is its region of convergence in the $z_1,z_2$ plane. The properties of the two-dimensional $z$ transform are similar to the properties of the $z$ transform in one dimension.

If the sequence $x(m,n)$ is of finite duration and is bounded then (3) has finite limits in all the summations and $X(z_1,z_2)$ converges everywhere in the $z_1z_2$ plane.

The two-dimensional $z$ transform of (2) can be shown [8] to be

$$A(z_1,z_2)F(z_1,z_2) = B(z_1,z_2)G(z_1,z_2)$$

or

$$G(z_1,z_2) = H(z_1,z_2)F(z_1,z_2)$$

where $F(z_1,z_2)$ and $G(z_1,z_2)$ are the two-dimensional $z$ transforms of the input and the output sequences of the filter, respectively, and

$$H(z_1,z_2) = \frac{A(z_1,z_2)}{B(z_1,z_2)} \triangleq \frac{\sum_{i=1}^{M_a} \sum_{j=1}^{N_a} a_{ij} z_1^{i-1} z_2^{j-1}}{\sum_{i=1}^{M_b} \sum_{j=1}^{N_b} b_{ij} z_1^{i-1} z_2^{j-1}} \tag{4}$$

is the transfer function of the filter. The frequency response of the filter is obtained by evaluating (4) for $z_1 = \exp(-j\omega_1 X)$ and $z_2 = \exp(-j\omega_2 Y)$, where $X$ and $Y$ are the sample intervals in the $x$ and $y$ directions, respectively.

The transfer function $H(z_1,z_2)$ given in (4) can be associated with the recursive filters recursing in the directions $(-m,n)$, $(m,-n)$, and $(-m,-n)$ by changing $z_1$ by $z_1^{-1}$, $z_2$ by $z_2^{-1}$, or both, respectively.

## III. DESIGN OF ROTATED FILTERS

Suppose a one-dimensional continuous filter whose impulse response is real, is given in its factored form

$$H_1(s) = H_0\Big[\prod_{i=1}^{m} (s - q_i) \Big/ \prod_{i=1}^{n} (s - p_i)\Big] \tag{5}$$

where $H_0$ is a scalar gain constant. The zero locations $q_i$ and the pole locations $p_i$ may be complex, in which case their conjugates are also present in the corresponding product. Assume that this filter has unity cutoff angular frequency.

The filter given in (5) can also be viewed as a two-dimensional filter that varies in one dimension only and could be written as follows:

[1] Some authors use an equivalent definition by replacing the unit delay operators $z_1$ and $z_2$ in (3) by $z_1^{-1}$ and $z_2^{-1}$, respectively. We use the definition in (3) because it is more common in the two-dimensional recursive filter literature [6], [7].

$$H_2(s_1,s_2) = H_1(s_2) = H_0\Big[\prod_{i=1}^{m} (s_2 - q_i) \Big/ \prod_{i=1}^{n} (s_2 - p_i)\Big]. \tag{6}$$

Rotating clockwise the $(s_1,s_2)$ axes through an angle $\beta$ by means of the transformation (7) we obtain the filter of (8), whose frequency response is rotated by an angle $-\beta$ with respect to the frequency response of (6)

$$s_1 = s_1' \cos\beta + s_2' \sin\beta \tag{7a}$$

$$s_2 = -s_1' \sin\beta + s_2' \cos\beta \tag{7b}$$

$$H_2(s_1',s_2') = H_0 \frac{\prod_{i=1}^{m} [(s_2' \cos\beta - s_1' \sin\beta) - q_i]}{\prod_{i=1}^{n} [(s_2' \cos\beta - s_1' \sin\beta) - p_i]}. \tag{8}$$

$H_2(s_1',s_2')$ describes a continuous two-dimensional filter in the new coordinate system of $s_1'$ and $s_2'$. To produce the corresponding two-dimensional discrete filter we use the two-dimensional bilinear $z$ transform [6] defined by the following two equations:

$$s_1' = \frac{2}{T}\frac{1 - z_1}{1 + z_1} \tag{9a}$$

$$s_2' = \frac{2}{T}\frac{1 - z_2}{1 + z_2}. \tag{9b}$$

It is assumed throughout the study that the sample interval $T$ is the same in both directions. Substituting (9) into (8) we obtain

$$H(z_1,z_2) = A \prod_{i=1}^{M} \frac{a_{11}^i + a_{21}^i z_1 + a_{12}^i z_2 + a_{22}^i z_1 z_2}{b_{11}^i + b_{21}^i z_1 + b_{12}^i z_2 + b_{22}^i z_1 z_2} \tag{10}$$

where

$$\left.\begin{array}{ll}
A = H_0(\tfrac{1}{2}T)^{n-m} & \\
M = \max(m,n) & \\
\left.\begin{array}{l}
a_{11}^i = \cos\beta - \sin\beta - \tfrac{1}{2}Tq_i \\
a_{21}^i = \cos\beta + \sin\beta - \tfrac{1}{2}Tq_i \\
a_{12}^i = -\cos\beta - \sin\beta - \tfrac{1}{2}Tq_i \\
a_{22}^i = -\cos\beta + \sin\beta - \tfrac{1}{2}Tq_i
\end{array}\right\} & \text{for } 1 \le i \le m \\
a_{11}^i = a_{21}^i = a_{12}^i = a_{22}^i = 1, & \text{for } m < i \le M \\
\left.\begin{array}{l}
b_{11}^i = \cos\beta - \sin\beta - \tfrac{1}{2}Tp_i \\
b_{21}^i = \cos\beta + \sin\beta - \tfrac{1}{2}Tp_i \\
b_{12}^i = -\cos\beta - \sin\beta - \tfrac{1}{2}Tp_i \\
b_{22}^i = -\cos\beta + \sin\beta - \tfrac{1}{2}Tp_i
\end{array}\right\} & \text{for } 1 \le i \le n \\
b_{11}^i = b_{21}^i = b_{12}^i = b_{22}^i = 1, & \text{for } n < i \le M.
\end{array}\right\} \tag{11}$$

Equation (10) can be physically interpreted as a cascade of bilinear second-order systems and can be readily realized by complex cascade programming [8]. The operations are programmed using real arithmetic and are simplified using the fact that the impulse response of each pair of conjugate filters is real. The cascade form of two-dimensional recursive filters has some advantage over the direct form [9].

The desired cutoff frequency of the filter in (10) can be obtained by substituting in (11) $T$ by $\pi f_r$ or by $2 \tan (\pi/2) f_r$ if the frequency axis has to be prewarped [10, cf. eq. (9)] where $f_r$ is the desired cutoff frequency expressed as a fraction of the Nyquist frequency, that is

$$f_r = f/f_N$$

where $f_N \triangleq 1/2T$ is the Nyquist frequency.

Examples of rotated filters are given in Figs. 1 and 2. These figures show contour maps of the magnitude responses of a second-order Butterworth filter rotated through 0° and 285°, respectively. Frequencies are shown as fractions of the Nyquist frequency and in every case the magnitude response has been normalized to a peak response of 1.0, the contour interval is 0.1, and the cutoff frequency is 0.2.

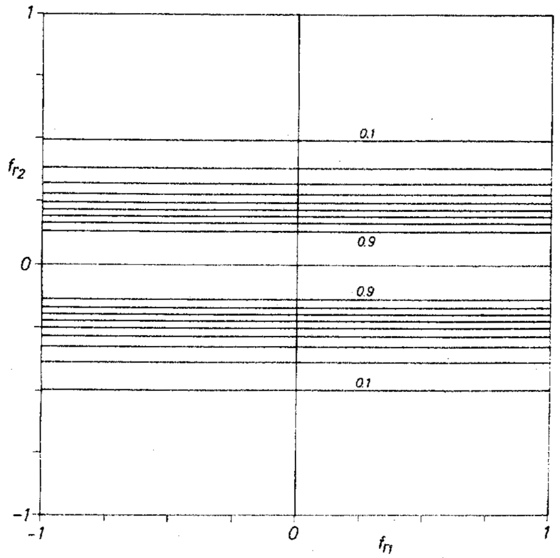


Fig. 1. Contour plot of the two-dimensional magnitude response of a second-order Butterworth filter rotated 0°.

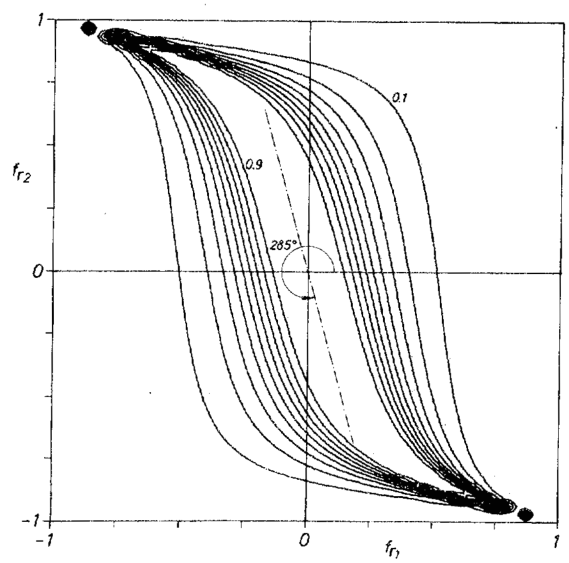


Fig 2. Contour plot of the two-dimensional magnitude response of second-order Butterworth filter rotated 285°.

## IV. STABILITY OF ROTATED FILTERS

Some basic theorems concerning stability of two-dimensional recursive filters are reviewed in Appendix A. Using Theorem 3 the conditions that the coefficients in (10) must satisfy to ensure the stability of the filter were derived. The results are given in the following two corollaries.

*Corollary 1*

A causal recursive filter with transfer function[2]

$$H(z_1,z_2) = \prod_{i=1}^{N} H_i(z_1,z_2) H_i^*(z_1^*,z_2^*) \tag{12}$$

where

$$H_i(z_1,z_2) = A_i(z_1,z_2)/B_i(z_1,z_2),$$

$A_i(z_1,z_2)$, and $B_i(z_1,z_2)$ $i = 1,2,\cdots,N$, are complex polynomials in $z_1$ and $z_2$ (for those $A_i$ and $B_i$ with real coefficients the complex conjugate factor $H_i^*(z_1^*,z_2^*)$ is set to unity), and $B_i(z_1,z_2)$ is of the form

$$B_i(z_1,z_2) = b_{11}{}^i + b_{21}{}^i z_1 + b_{12}{}^i z_2 + b_{22}{}^i z_1 z_2$$

is stable if

$$\big|\, |b_{21}{}^i b_{22}{}^{i*} - b_{11}{}^i b_{12}{}^{i*}| - |b_{11}{}^i b_{22}{}^i - b_{21}{}^i b_{12}{}^i| \,\big| > \big|\, |b_{12}{}^i|^2 - |b_{22}{}^i|^2 \,\big| \tag{13}$$

and

$$|b_{11}{}^i| > |b_{21}{}^i| \tag{14}$$

for $i = 1,2,\cdots,N$.

*Proof:* We want to show that for the class of filters specified in this corollary, (13) and (14) are equivalent to the "if" part of Theorem 3 in Appendix A.

Setting $B_i(z_1,z_2) = 0$ we obtain

$$z_2 = -\frac{b_{11}{}^i + b_{21}{}^i z_1}{b_{12}{}^i + b_{22}{}^i z_1} \triangleq f_i(z_1) \tag{15}$$

which is a bilinear transformation mapping circles into circles.[3]

Clearly, for the filter $H_i(z_1,z_2)$ condition 1) of Theorem 3 is satisfied if and only if

$$\big|\, |c_i| - r_i \,\big| > 1 \tag{16}$$

where $c_i$ is the center and $r_i$ is the radius of the circle image of the unit circle by the transformation $z_2 = f_i(z_1)$.

[2] The * denotes complex conjugate.

[3] Here we include straight lines as circles with infinite radii.

We have derived expressions for $c_i$ and $r_i$ as a function of the filter coefficients in Lemma 1 of Appendix B.

But (16) is equivalent to (13) by substituting (B2) and (B3) into (16), that is

$$\left| \left| \frac{b_{21}{}^i b_{22}{}^{i*} - b_{11}{}^i b_{12}{}^{i*}}{|b_{12}{}^i|^2 - |b_{22}{}^i|^2} \right| - \left| \frac{b_{11}{}^i b_{22}{}^i - b_{21}{}^i b_{12}{}^i}{|b_{12}{}^i|^2 - |b_{22}{}^i|^2} \right| \right| > 1$$

which is equivalent to (13).

For condition 2) consider the inverse transformation

$$z_1 = f_i^{-1}(z_2) = -\frac{b_{11}{}^i + b_{12}{}^i z_2}{b_{21}{}^i + b_{22}{}^i z_2}$$

$$\hat{z}_1 \triangleq f_i^{-1}(z_2)\,|_{z_2=0} = -b_{11}{}^i / b_{21}{}^i. \tag{17}$$

Therefore, for the filter $H_i(z_1,z_2)$ the second condition of Theorem 3 is verified if and only if $|\hat{z}_1| > 1$, that is

$$|-b_{11}{}^i/b_{21}{}^i| > 1$$

which is equivalent to (14).

Since (13) and (14) compare magnitudes only, the same conditions apply to $H_i(z_1,z_2)$ and $H_i^*(z_1^*,z_2^*)$; therefore, in general (13) and (14) have to be checked for $i = 1,2,\cdots,N = (M + N_r)/2 \leq M$ only, where $N_r$ is the number of filters $H_i(z_1,z_2)$ with real coefficients and $M$ is the total number of filters $H_i(z_1,z_2)$ in the cascade.

If every filter $H_i(z_1,z_2)$ in the cascade is stable, then clearly the filter $H(z_1,z_2)$ is stable. Q.E.D.

Specializing Corollary 1 to rotated filters with their coefficients as defined in (11) we obtain Corollary 2.

*Corollary 2*

Rotating a stable one-dimensional continuous filter by an angle $\beta$ in the $(s_1,s_2)$ plane and applying the two-dimensional bilinear $z$ transform, the resulting two-dimensional digital filter [cf. (10)] is stable if $270° \leq \beta \leq 360°$.

*Proof:* Substituting (11) into (13) and (14) we obtain (18) and (19) as sufficient stability conditions for rotated filters

$$||a_i| - |\cos\beta|| > |a_i + \cos\beta| \tag{18}$$

$$|\cos\beta - \sin\beta - a_i| > |\cos\beta + \sin\beta - a_i|, \quad \text{for } i = 1,2,\cdots,M \tag{19}$$

where $a_i = \mathrm{Re}\,[(T/2)p_i]$ and $p_i$ represents the location of a pole.

There are no values of $a_i$ and $\beta$ satisfying (18); at best, both sides of (18) are equal. This is because the transformation $B_i(z_1,z_2) = 0$ has a fixed point at $z_1 = z_2 = -1$ (the other fixed point of the transformation is $-b_{11}/b_{22}$). This pole is cancelled by a zero because the transformation $A_i(z_1,z_2) = 0$ has also a fixed point at $z_1 = z_2 = -1$. However, the pole and zero might not exactly cancel each other because of quantization. To avoid this, since the center of the circle image lies on the real axis (see the corollary in Appendix B), we can always shift the circle image to the left by a small distance $\epsilon$. This is illustrated in Fig. 3. This displacement eliminates the overlapping of the two circles at the point $z_1 = z_2 = -1$. However, in all the filters that we have designed using the rotation procedure there was never a need for this shift because the impulse responses decayed sufficiently quickly.

The set of values that satisfy (18) with equality is[4]

$$S_i = \{a_i,\beta: (a_i < 0 \cap \cos\beta > 0) \cup (a_i > 0 \cap \cos\beta < 0)\}.$$

The set of values that satisfy (19) is

$$S_2 = \{a_i,\beta: (\sin\beta > 0 \cap a_i > \cos\beta) \cup (\sin\beta < 0 \cap a_i < \cos\beta)\}.$$

The set of values of $a_i$ and $\beta$ for which rotated filters are stable is given by the intersection of set $S_1$ and set $S_2$.

$$S_1 \cap S_2 = \{a_i,\beta: (a_i < 0 \cap 270° < \beta < 360°) \cup (a_i > 0 \cap 90° < \beta < 180°)\}.$$

The regions of stability are illustrated in Fig. 4.

For $\beta = 270°$ and $\beta = 360°$ the bilinear transformation in (15) is degenerate. However, in these cases the two-dimensional filter varies in one dimension only and it can easily be shown that it is stable provided that the one-dimensional filter has all its poles in the LHP (left-hand plane).

Therefore, for stability $a_i < 0$, $i = 1,2,\cdots,M$, and $270° \leq \beta \leq 360°$. Q.E.D.

Theorem 4 in Appendix A indicates that it might be possible to obtain stable filters for other angles of rotation by changing the direction of recursion. That is, by substituting either $z_1$ by $z_1^{-1}$, or $z_2$ by $z_2^{-1}$, or both, in the filter transfer function $H(z_1,z_2)$.

The application of Corollary 1 to all cases of interest results in Table I. Nevertheless, all the possibilities indicated by Table I result in a filter with the same magnitude response, that is, the effective angle of rotation always satisfies $270° < \beta_e < 360°$. To obtain a rotation through a different angle the data can be filtered in a distinct manner. Consider for example the following.

In the frequency domain the filtering operation can be represented as

$$\begin{aligned} G[\exp(-j\omega_1 T), \exp(-j\omega_2 T)] &= H[\exp(-j\omega_1 T), \exp(-j\omega_2 T)] \\ &\quad \cdot F[\exp(-j\omega_1 T), \exp(-j\omega_2 T)]. \end{aligned} \tag{20}$$

It is easy to see that a rotation of the filter transfer function $H[\exp(-j\omega_1 T), \exp(-j\omega_2 T)]$ by an angle $\theta$ is equivalent to a rotation of the two-dimensional Fourier transform of the two-dimensional input signal $F[\exp(-j\omega_1 T), \exp(-j\omega_2 T)]$ by an angle $-\theta$ and a rotation of the output by an angle $\theta$. Since the rotation of a function of two variables in the space domain causes an equal rotation of its Fourier transform in the frequency domain [8], to obtain a filter rotated by an angle $\beta$, when $0° < \beta < 270°$, we may rotate the matrix contain-

[4] ∩ means "and" and ∪ means "or."

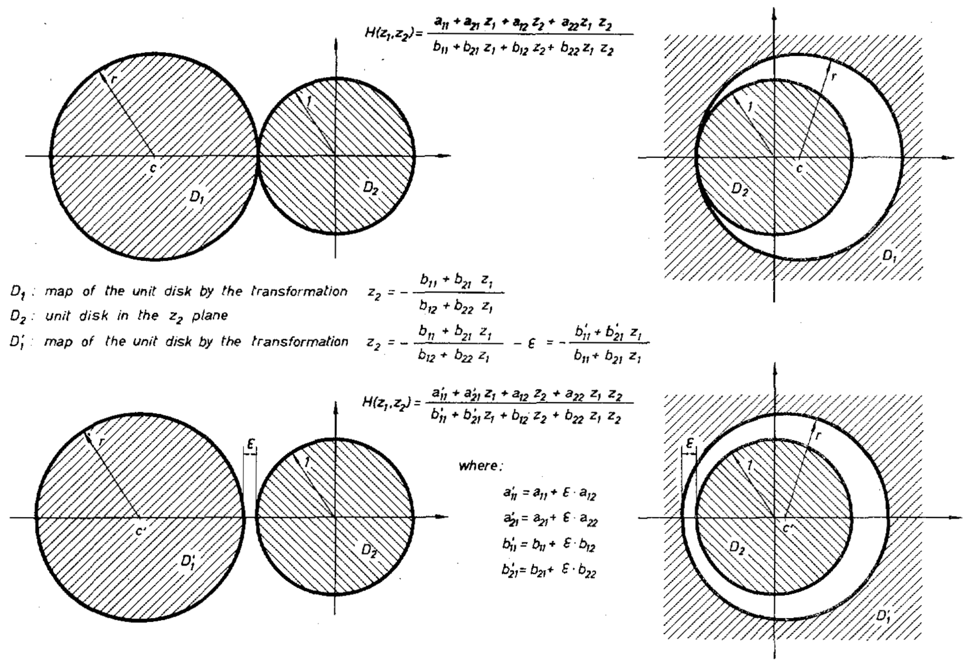


Fig. 3. Stabilization of marginally unstable rotated filters.

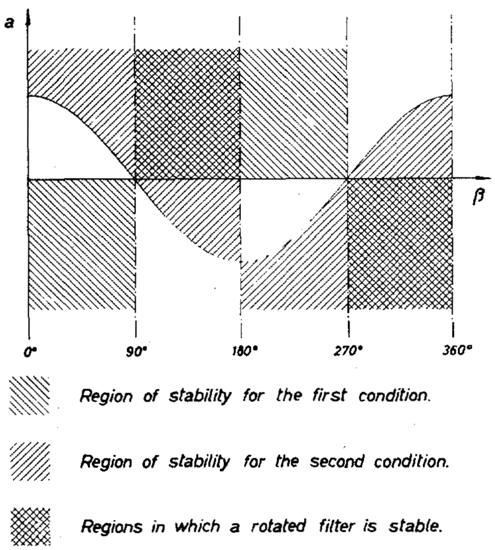


Fig. 4. Regions of stability for rotated filters with transfer function $H(z_1, z_2)$.

TABLE I
STABILITY REGIONS FOR ROTATED FILTERS

| Transfer function of the two-dimensional filter | Location of the poles of the original one-dimensional filter H(s) | |
|---|---|---|
| | L.H.P. | R.H.P |
| $H(z_1,z_2)$ | $270^\circ < \beta < 360^\circ$ | $90^\circ < \beta < 180^\circ$ |
| $H(z_1^{-1},z_2)$ | $0^\circ < \beta < 90^\circ$ | $180^\circ < \beta < 270^\circ$ |
| $H(z_1,z_2^{-1})$ | $180^\circ < \beta < 270^\circ$ | $0^\circ < \beta < 90^\circ$ |
| $H(z_1^{-1},z_2^{-1})$ | $90^\circ < \beta < 180^\circ$ | $270^\circ < \beta < 360^\circ$ |

ing the input data by $-90^\circ$, $-180^\circ$, or $-270^\circ$, rotate the filter by $\beta_f$, where $270^\circ \leq \beta_f \leq 360^\circ$ for stability, perform the filtering operation and finally rotate the output matrix to the original position. Since the data are usually given in the form of a matrix, which allows us to perform the digital filtering operation, it can be easily rotated by angles which are multiples of 90°.

When choosing the angles of rotation for the data and for the filter the following equation has to be satisfied

$$\beta_e = \beta_f - \beta_d \tag{21}$$

where

- $\beta_e$ effective angle of rotation of the filter with respect to the original data matrix;
- $\beta_f$ angle of rotation of the filter ($270^\circ \leq \beta_f \leq 360^\circ$ for stability);
- $\beta_d$ $k90^\circ$ = angle of rotation of the input data matrix ($k$ is an integer).

Thus, given $\beta_e$, the appropriate value of $k$ has to be chosen such that $\beta_f = \beta_e + k90^\circ$ and $270^\circ \leq \beta_f \leq 360^\circ$ are satisfied. Note that all the angles are measured counter-clockwise and modulo 360°, so $k \geq 0$ because $\beta_f \geq \beta_e$ always. After filtering, the output matrix has to be rotated by an angle $-\beta_d$. A block diagram of this technique is given in Fig. 5(a), where $R$ denotes a rotation by $\beta_d$ and $H$ denotes a $\beta_f$-rotated filter. The system is equivalent to a $\beta_e$-rotated filter with $\beta_e = \beta_f - \beta_d$.

The rotation of the data is not the only possible solution. There are other transformations of the data which change the direction of recursion. These transformations are the matrix transposition with respect to each diagonal

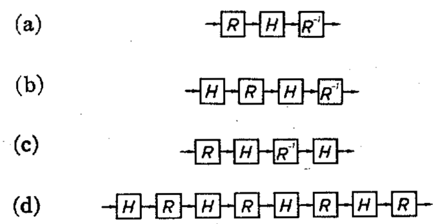


Fig. 5. Realization of noncausal filters by combining data rotations with a causal filter.

and the horizontal and vertical mirror images. An alternative solution to the transformation of the data may be obtained by using algorithms recursing in other directions (noncausal filters).

## V. DESIGN OF FILTERS WITH CIRCULAR SYMMETRY

We have shown that stable rotated filters can be obtained for any effective angle of rotation ($\beta_e$). Therefore, cascading a number of rotated filters whose angles of rotation are uniformly distributed over 180° results in a magnitude response which approximates a circularly symmetric function by a polygonal. This polygonal has an even number of sides because with each rotated filter we obtain two sides of the polygonal. The more filters that are cascaded, the more sides the polygonal has and the better the circular symmetry.

Suppose that the angles of rotation are between 180° and 360°. When the angle of rotation is $\beta$, $180° < \beta < 270°$, we have to transform the data matrix according to what was said in Section IV, then filter with a $\beta + 90°$ rotated filter, and inverse-transform the output matrix. If $\beta$ is distributed between 180° and 360°, these filters rotated by $\beta + 90°$, $180° < \beta < 270°$, coincide with those rotated by $\beta$, $270° < \beta < 360°$. Therefore, we need a filter consisting of rotated filters whose angles of rotation are distributed between 270° and 360°. The contour levels of the magnitude response of that filter have approximately elliptical shapes with major axis oriented 315°. We refer to this class of filters as elliptically shaped filters. Fig. 6 shows an example of an elliptically shaped filter obtained by cascading three second-order Butterworth filters rotated by 285°, 315°, and 345° and cutoff frequency 0.2. To obtain a circularly symmetric magnitude response the sequence of operations indicated in Fig. 5(b) is used, where $H$ denotes the elliptically shaped filter and $R$ denotes a data rotation by 90°. Here we assume that the impulse response of the elliptically shaped filter becomes negligible fast enough with respect to the dimensions of the data. An alternative solution is shown in Fig. 5(c).

The combination shown in Fig. 5(a) with $R$ a rotation by 90° and $H$ an elliptical filter is equivalent to an elliptically shaped filter with major axis oriented 225°. The magnitude response of this filter is shown in Fig. 7. Cascading the filters in Figs. 6 and 7 we obtain the filter

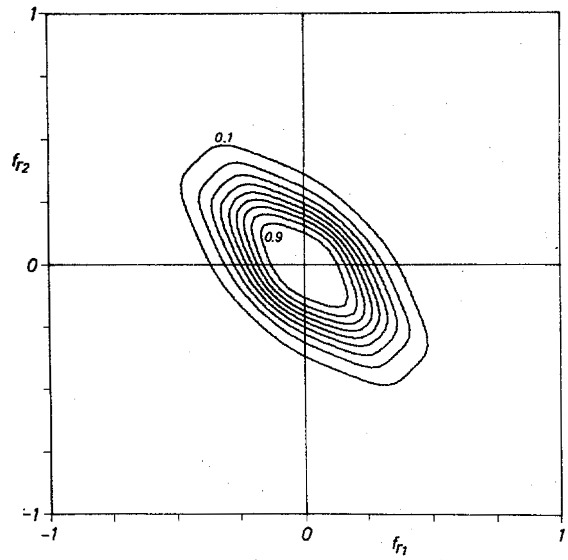


Fig. 6. Contour plot of the two-dimensional magnitude response of a cascade of three second-order Butterworth filters rotated 285°, 315°, and 345°.

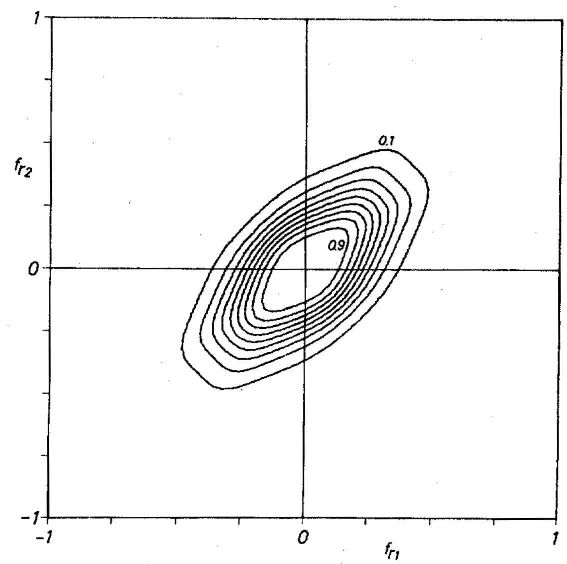


Fig. 7. Contour plot of the two-dimensional magnitude response of a cascade of three second-order Butterworth filters rotated 195°, 225°, and 255°.

shown in Fig. 8. A fine detail in one quadrant of the same magnitude response is shown in Fig. 11.

Figs. 9 through 11 show the magnitude responses obtained by cascading 2, 4, and 6 rotated filters, respectively. We observe that cascading more than four rotated filters the polygonal shape of the contour levels cannot be appreciated. Note also that as the number of rotated filters which are cascaded increases, the attenuation also increases and the cutoff region becomes steeper.

Two-dimensional filters with zero-phase response can be obtained [6]. Suppose, for example, that the linear operation indicated in Fig. 5(d) is performed, where $H$ denotes an elliptically shaped filter with major axis

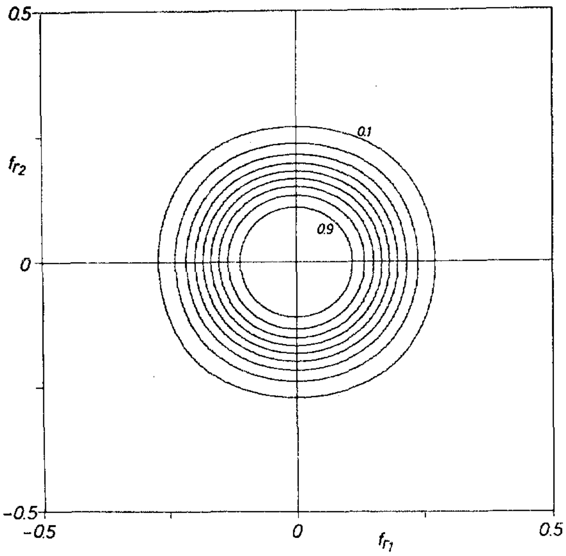


Fig. 8. Contour map of the two-dimensional magnitude response of the composite filter formed by cascading the two filters whose magnitude responses are shown in Figs. 6 and 7.

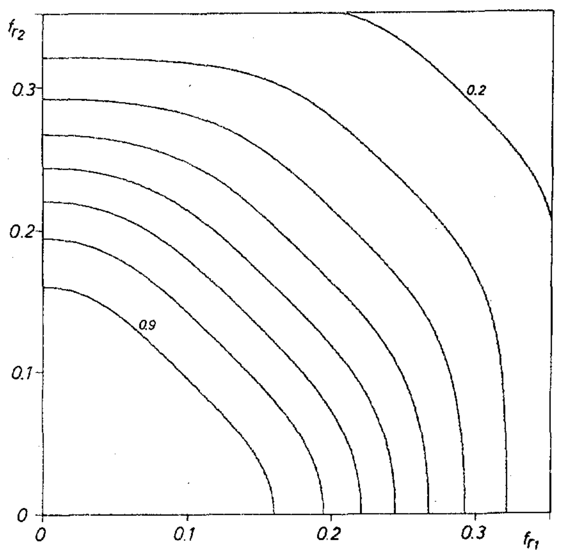


Fig. 9. Contour plot of the two-dimensional magnitude response of a cascade of two second-order Butterworth filters rotated 225° and 315°.

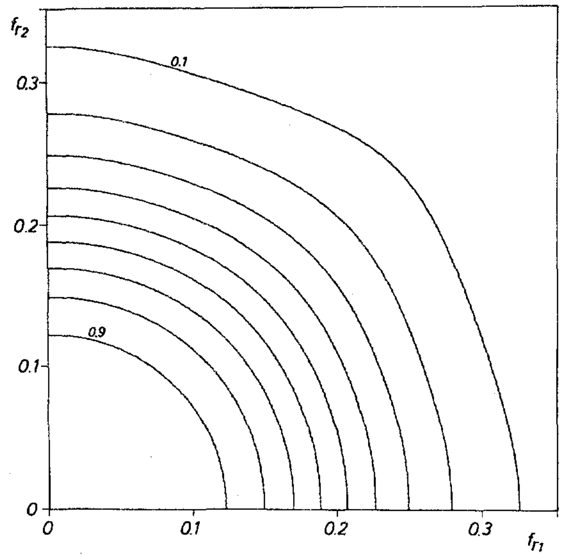


Fig. 10. Contour plot of the two-dimensional magnitude response of a cascade of four second-order Butterworth filters rotated by multiples of 45°.

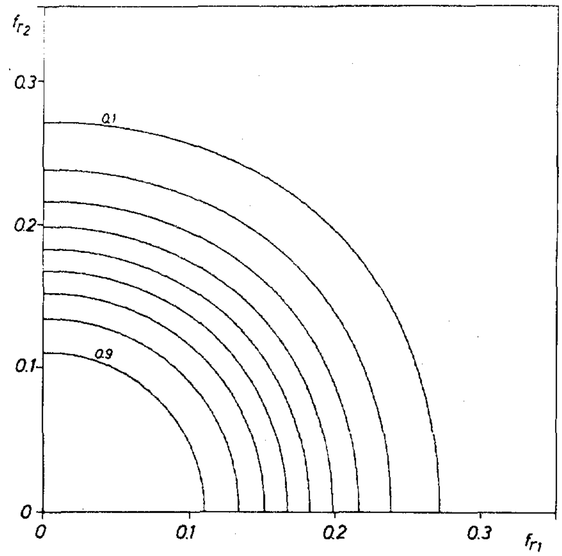


Fig. 11. Contour plot of the two-dimensional magnitude response of a cascade of six second-order Butterworth filters rotated by multiples of 30°.

oriented 315° and $R$ denotes a rotation by 90°. This is equivalent to a cascade of an even number of rotated filters whose angles of rotation are uniformly distributed between 0° and 360°. This filter has zero-phase response. Indeed, its transfer function can be written as follows:

$$\hat{H}(z_1,z_2) = H(z_1,z_2)H(z_1^{-1},z_2^{-1})$$

where $H(z_1,z_2)$ is the transfer function of a cascade of rotated filters whose angles of rotation are distributed over 180°. Clearly, the filter $\hat{H}(z_1,z_2)$ has zero-phase response and its magnitude response is the square of the magnitude response of $H(z_1,z_2)$.

## VI. CHOICE OF FILTER PARAMETERS

In the previous section it was pointed out that the cutoff frequency and the shape of the magnitude response of a two-dimensional filter depend on the number of rotated filters being cascaded. In this section we show briefly how these parameters can be controlled.

### A. *Cutoff Frequency*

The technique used to obtain a two-dimensional filter with a specified cutoff frequency in a given direction consists of an iteration that modifies the cutoff frequency of the original one-dimensional continuous filter in the proper amount and sense until the desired cutoff frequency of the two-dimensional digital filter is reached.

This method was implemented by writing a program in Fortran IV featuring the following steps.

1) Read in the coefficients of the one-dimensional continuous filter (with cutoff angular frequency normalized to unity), the number of rotations desired, and the de-

sired cutoff frequency $f_u$ of the two-dimensional digital filter given as a fraction of the Nyquist frequency.

2) Determine the coefficients of a two-dimensional digital filter [using (11)] derived from a one-dimensional filter with cutoff frequency $f_u$.

3) Find the cutoff frequency $f_c$ of the filter obtained in a given direction.

4) Determine the coefficients of a two-dimensional digital filter derived from a one-dimensional filter with cutoff frequency $f_d = 2f_u - f_c$.

5) Repeat steps 3) and 4) until $|f_u - f_c| < \epsilon$ where $\epsilon$ is the specified maximum error of the cutoff frequency in that direction.

6) Determine the shape factors (see Section VI-B).

7) Check for stability.

8) Evaluate the magnitude response and plot a contour map.

The program described previously was used to design many filters of different shapes and cutoff frequencies. The convergence was obtained quickly. The number of iterations required increases with the cutoff frequency and decreases with the order of the original one-dimensional filter.

### B. Shape Factors

Shape factors will be used here as a measurement of how good a filter is. Rather than giving large tables of shape factors for various classes of filters, we describe some different kinds of shape factors that are suitable for two-dimensional digital filters. We also give some tables containing shape factors of two-dimensional recursive filters derived from Butterworth filters of different orders. Since the shape of the magnitude response of a filter depends on the cutoff frequency, all these tables are given for filters normalized to a cutoff frequency of 0.1. Different kinds of shape factors are shown in Fig. 12.

The first shape factor is the ratio in decibels of the magnitude response at the cutoff frequency and the magnitude response at a frequency at a distance $d$ beyond the cutoff frequency in a specified direction. This shape factor, that we call shape factor number 1, is given in Table II for $d = 0.05$ in the directions 0° and 45°.

The second shape factor (No. 2) is the distance between the cutoff frequency and the frequency corresponding to an attenuation of $A$ dB. Table III gives this shape factor for $A = 40$ in the directions 0° and 45°.

The third shape factor (No. 3) concerns the circular symmetry only and gives the area between the $-3$-dB contour and a circle of radius the cutoff frequency. These areas are given in Table IV.

The fourth shape factor (No. 4) is both a measure of the steepness of the magnitude response and a measure of the circular symmetry. It gives the volume (see Table V) between the magnitude response of the filter and the magnitude response of an ideal filter (low-pass). The magnitude response of an ideal low-pass two-dimensional filter in polar coordinates is

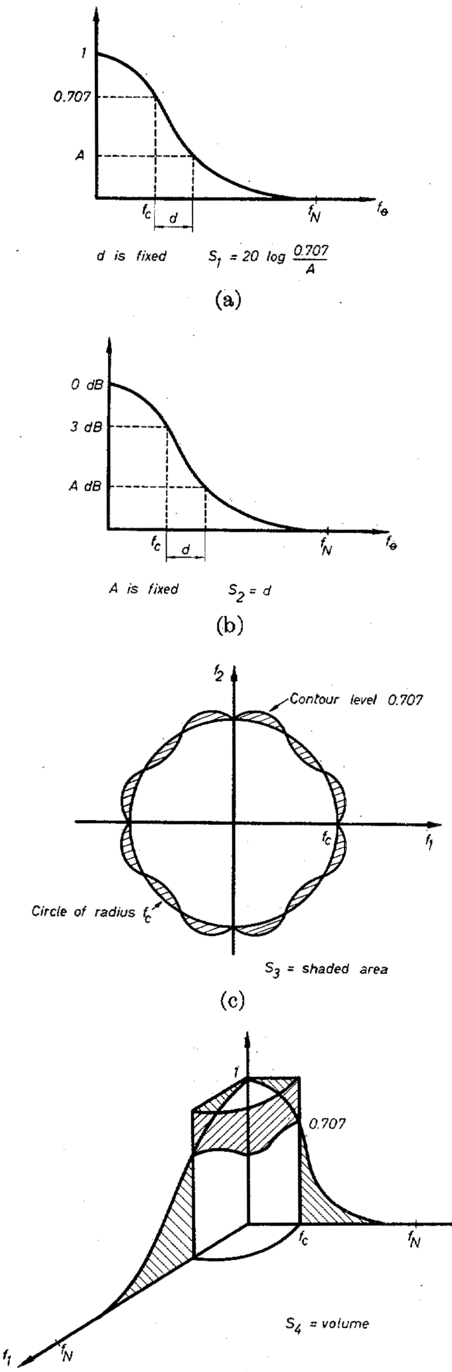


Fig. 12. Shape factors.

$$H(\nu) = \begin{cases} 1 & \text{for } \nu < f_c \\ 0 & \text{otherwise.} \end{cases}$$

From the observation of the tabulated results, the following general conclusions can be made.

The steepness of the filter is highly dependent on the number of rotated filters being cascaded, the type of one dimensional filters used, and the order of the filters. Shape factors 1 and 2 indicate the steepness of the filter, usually considered the main criterion for low-pass filters. In one dimension, the steepness of the filter is well known if given

TABLE II
SHAPE FACTOR NUMBER 1 (IN DECIBELS)

| Order of Butterworth filter | Number of rotated filters being cascaded | | | | | |
|---|---|---|---|---|---|---|
| | 2 | 4 | 6 | 8 | 10 | 12 |
| | $d=0.05$ $\theta=0^\circ$ | | | | | |
| 1 | 2.80 | 3.05 | 3.28 | 3.41 | 3.50 | 3.56 |
| 2 | 7.06 | 7.34 | 8.56 | 9.26 | 9.77 | 10.15 |
| 3 | 12.59 | 12.75 | 15.56 | 17.54 | 19.10 | 20.36 |
| 4 | 18.96 | 19.04 | 23.48 | 27.53 | 30.80 | 33.63 |
| 5 | 25.78 | 25.82 | 31.75 | 38.51 | 43.92 | 48.86 |
| 6 | 32.83 | 32.84 | 40.15 | 49.98 | 57.72 | 65.15 |
| 7 | 39.98 | 39.98 | 48.60 | 61.67 | 71.82 | 81.99 |
| 8 | 47.17 | 47.17 | 57.10 | 73.43 | 86.05 | 99.07 |
| 9 | 54.38 | 54.38 | 65.65 | 85.20 | 100.30 | 116.27 |
| 10 | 61.59 | 61.60 | 74.26 | 96.94 | 114.53 | 133.49 |
| | $d=0.05$ $\theta=45^\circ$ | | | | | |
| 1 | 1.95 | 2.99 | 3.21 | 3.34 | 3.32 | 3.48 |
| 2 | 5.50 | 7.17 | 8.34 | 9.02 | 9.51 | 9.87 |
| 3 | 9.71 | 12.46 | 15.12 | 17.05 | 18.54 | 19.74 |
| 4 | 14.19 | 18.61 | 23.05 | 26.76 | 29.91 | 32.60 |
| 5 | 18.79 | 25.26 | 31.62 | 37.46 | 42.70 | 47.41 |
| 6 | 23.42 | 32.16 | 40.48 | 48.66 | 56.26 | 63.27 |
| 7 | 28.06 | 39.18 | 49.46 | 60.09 | 70.20 | 79.70 |
| 8 | 32.72 | 46.25 | 58.44 | 71.60 | 84.32 | 96.39 |
| 9 | 37.37 | 53.34 | 67.37 | 83.13 | 98.50 | 113.20 |
| 10 | 42.02 | 60.44 | 76.25 | 94.64 | 112.70 | 130.04 |

TABLE III
SHAPE FACTOR NUMBER 2

| Order of Butterworth filter | Number of rotated filters being cascaded | | | | | |
|---|---|---|---|---|---|---|
| | 2 | 4 | 6 | 8 | 10 | 12 |
| | $A=40$ $\theta=0^\circ$ | | | | | |
| 1 | 0.6532 | 0.4694 | 0.3967 | 0.3545 | 0.3288 | 0.3120 |
| 2 | 0.2546 | 0.2007 | 0.1565 | 0.1371 | 0.1264 | 0.1194 |
| 3 | 0.1392 | 0.1283 | 0.0951 | 0.0843 | 0.0775 | 0.0731 |
| 4 | 0.0937 | 0.0920 | 0.0694 | 0.0614 | 0.0564 | 0.0531 |
| 5 | 0.0702 | 0.0699 | 0.0558 | 0.0486 | 0.0447 | 0.0420 |
| 6 | 0.0559 | 0.0559 | 0.0471 | 0.0405 | 0.0372 | 0.0349 |
| 7 | 0.0465 | 0.0465 | 0.0412 | 0.0349 | 0.0320 | 0.0300 |
| 8 | 0.0397 | 0.0397 | 0.0366 | 0.0308 | 0.0281 | 0.0263 |
| 9 | 0.0346 | 0.0346 | 0.0329 | 0.0277 | 0.0252 | 0.0236 |
| 10 | 0.0307 | 0.0307 | 0.0298 | 0.0253 | 0.0228 | 0.0214 |
| | $A=40$ $\theta=45^\circ$ | | | | | |
| 1 | 0.8898 | 0.5498 | 0.4541 | 0.3944 | 0.3622 | 0.3414 |
| 2 | 0.6127 | 0.2117 | 0.1619 | 0.1422 | 0.1308 | 0.1234 |
| 3 | 0.2800 | 0.1329 | 0.0992 | 0.0865 | 0.0794 | 0.0748 |
| 4 | 0.1661 | 0.0945 | 0.0720 | 0.0628 | 0.0575 | 0.0542 |
| 5 | 0.1149 | 0.0716 | 0.0565 | 0.0496 | 0.0455 | 0.0427 |
| 6 | 0.0869 | 0.0571 | 0.0466 | 0.0412 | 0.0378 | 0.0355 |
| 7 | 0.0696 | 0.0473 | 0.0399 | 0.0355 | 0.0325 | 0.0305 |
| 8 | 0.0578 | 0.0404 | 0.0351 | 0.0313 | 0.0286 | 0.0268 |
| 9 | 0.0494 | 0.0352 | 0.0315 | 0.0282 | 0.0257 | 0.0239 |
| 10 | 0.0431 | 0.0312 | 0.0288 | 0.0257 | 0.0233 | 0.0217 |

TABLE IV
SHAPE FACTOR NUMBER 3 ($\times 10^{-6}$)

| Order of Butterworth filter | Number of rotated filters being cascaded | | | | | |
|---|---|---|---|---|---|---|
| | 2 | 4 | 6 | 8 | 10 | 12 |
| 1 | 4.38 | 0.19 | 0.14 | 0.23 | 0.21 | 0.20 |
| 2 | 6.02 | 0.32 | 0.14 | 0.14 | 0.16 | 0.16 |
| 3 | 16.14 | 1.94 | 0.34 | 0.16 | 0.21 | 0.16 |
| 4 | 27.15 | 1.09 | 0.40 | 0.12 | 0.32 | 0.97 |
| 5 | 38.08 | 0.19 | 0.67 | 0.13 | 0.16 | 0.21 |
| 6 | 48.90 | 1.73 | 1.05 | 0.40 | 0.22 | 0.37 |
| 7 | 59.69 | 3.72 | 1.24 | 0.44 | 0.16 | 0.19 |
| 8 | 70.15 | 5.47 | 1.02 | 0.56 | 0.37 | 0.84 |
| 9 | 81.00 | 7.24 | 1.03 | 0.95 | 0.83 | 0.37 |
| 10 | 90.93 | 9.25 | 0.20 | 1.02 | 0.78 | 0.85 |

TABLE V
SHAPE FACTOR NUMBER 4 ($\times 10^{-2}$)

| Order of Butterworth filter | Number of rotated filters being cascaded | | | | | |
|---|---|---|---|---|---|---|
| | 2 | 4 | 6 | 8 | 10 | 12 |
| 1 | 17.65 | 12.09 | 9.98 | 8.92 | 8.31 | 7.93 |
| 2 | 4.53 | 3.90 | 3.16 | 2.88 | 2.72 | 2.62 |
| 3 | 2.34 | 2.24 | 1.86 | 1.71 | 1.62 | 1.56 |
| 4 | 1.55 | 1.53 | 1.33 | 1.21 | 1.15 | 1.11 |
| 5 | 1.15 | 1.14 | 1.03 | 0.94 | 0.89 | 0.86 |
| 6 | 0.90 | 0.90 | 0.84 | 0.76 | 0.72 | 0.69 |
| 7 | 0.73 | 0.73 | 0.70 | 0.64 | 0.60 | 0.57 |
| 8 | 0.61 | 0.61 | 0.59 | 0.54 | 0.50 | 0.48 |
| 9 | 0.51 | 0.51 | 0.50 | 0.46 | 0.42 | 0.40 |
| 10 | 0.43 | 0.43 | 0.42 | 0.39 | 0.36 | 0.33 |

the type of filter, such as Butterworth or Chebyshev, and the order of the filter. However, in two dimensions the number of rotated filters being cascaded also affects the steepness. Tables II and III show that the steepness of the filters is monotonically increasing with respect to both the order of the filter and the number of filter rotations. As a design criterion, the steepness of a filter increases more rapidly with the change of order than with the increase of the number of filters being cascaded. The effect of the number of filter rotations on steepness decreases as the number of rotations increases (the gain in steepness is the greatest when the filter is realized by a lower number of rotations).

In contrast to the monotonic relation of shape factors 1 and 2, shape factor 3, which indicates the exactness of the realized filter symmetry to the ideal circular symmetry, shows no simple relationship with respect to the two parameters considered. This shape factor varies in an erratic manner, although some general pattern can be noticed. The reason for this variation is that shape factor 3 is highly dependent on the direction chosen for the exact cutoff frequency. A fairer comparison between filters could be done if shape factors 3 and 4 were determined with filters whose cutoff frequency were exact in the optimum direction, that is in the direction in which shape factors 3 and 4 were minimized.

## VII. CONCLUSIONS

The work described previously concerns the design of stable two-dimensional recursive filters whose magnitude response approximates a circularly symmetric function. The principal advantages of the method are the following.

1) Stability can be guaranteed.

2) The method leads to a recursive realization which is more efficient than a nonrecursive one.

3) The filters are factorable into lower order filters, so that they can be efficiently realized. In general this factorization is not possible for two-dimensional recursive filters.

4) The calculation of the coefficients of a filter using a digital computer is fast.

Finally, we have shown how to obtain the desired cutoff frequency in a given direction with a specified maximum error in that direction. We have also given tables of shape factors to help the designer choosing the order of the original filter and the number of rotations for a particular application.

Future work could be done on frequency domain synthesis in order to have more control of the error from the ideal characteristics of the filter. In particular, a problem of interest is to choose a direction for the exact cutoff *frequency such that the deviation from the cutoff fre-*quency in all other directions is minimized (i.e., minimize shape factor number 3, see Section VI-B). The suitability of the filters discussed here for filtering images (or other practical applications) could be tested.

## APPENDIX A

The following theorems concern stability of two-dimensional recursive filters.

*Theorem 1* [11]

A two-dimensional filter is said to be stable (in the sense that a bounded input produces a bounded output) if and only if its impulse response satisfies the constraint

$$\sum_{m=-\infty}^{\infty} \sum_{n=-\infty}^{\infty} | h(m,n) | < \infty . \tag{A1}$$

*Theorem 2* [6], [7]

A causal recursive filter with transfer function

$$H(z_1,z_2) = A(z_1,z_2)/B(z_1,z_2)$$

where $A$ and $B$ are polynomials in $z_1$ and $z_2$, is stable if *and only if there are no values of $z_1$ and $z_2$ such that* $B(z_1,z_2) = 0$, $|z_1| \leq 1$ and $|z_2| \leq 1$.

*Theorem 3* [7]

A causal recursive filter with transfer function $H(z_1,z_2) = A(z_1,z_2)/B(z_1,z_2)$, where $A$ and $B$ are polynomials is stable if and only if the following.

1) The map of the unit circle of the $z_1$ plane, $\{z_1: |z_1| = 1\}$ into the $z_2$ plane, according to the equation $B(z_1,z_2) = 0$, lies outside the unit disk in the $z_2$ plane, $\{z_2: |z_2| \leq 1\}$.

2) No point in the unit disk of the $z_1$ plane $\{z_1: |z_1| \leq 1\}$ maps into the point $z_2 = 0$ by the relation $B(z_1,z_2) = 0$.

*Theorem 4* [7]

Among the four recursive filters which can be associated with $H(z_1,z_2) = A(z_1,z_2)/B(z_1,z_2)$, that is, $H(z_1,z_2)$ itself, $H(z_1^{-1},z_2)$, $H(z_1,z_2^{-1})$, and $H(z_1^{-1},z_2^{-1})$, at most one is stable.

## APPENDIX B

*Lemma 1*

The image of the unit circle $\{z_1: |z_1| = 1\}$ by a bilinear transformation of the type

$$z_2 = -\frac{b_{11} + b_{21}z_1}{b_{12} + b_{22}z_1} \tag{B1}$$

where $b_{11}$, $b_{21}$, $b_{12}$, and $b_{22}$ are any complex constants, is another circle in the $z_2$ plane of center $c$ and radius $r$ given by

$$c = \frac{b_{21}b_{22}^* - b_{11}b_{12}^*}{|b_{12}|^2 - |b_{22}|^2} \tag{B2}$$

$$r = \left| \frac{b_{11}b_{22} - b_{21}b_{12}}{|b_{12}|^2 - |b_{22}|^2} \right| . \tag{B3}$$

*Proof:* The proof that (B1) maps circles into circles can be found in any text on complex variables (see for example [12]) and will not be included here.

To find the center and the radius of the circle image we have to determine two points $z_{1A}$ and $z_{1B}$ over the unit circle $\{z_1: |z_1| = 1\}$ such that their images $z_{2A}$ and $z_{2B}$ are diametrically opposite (i.e., maximally far apart) over the circle image. Under these circumstances

$$c = \frac{z_{2A} + z_{2B}}{2} \tag{B4}$$

$$r = \left| \frac{z_{2A} - z_{2B}}{2} \right| . \tag{B5}$$

In order to see how we choose $z_{1A}$ and $z_{1B}$ we write (B1) as follows:

$$z_2 = -\frac{b_{11} + b_{21}z_1}{b_{12} + b_{22}z_1} = -\frac{b_{21}}{b_{22}} - \frac{b_{11} - (b_{21}/b_{22})b_{12}}{b_{12} + b_{22}z_1}$$

$$= \mu + \frac{\nu}{b_{12} + b_{22}z_1} \tag{B6}$$

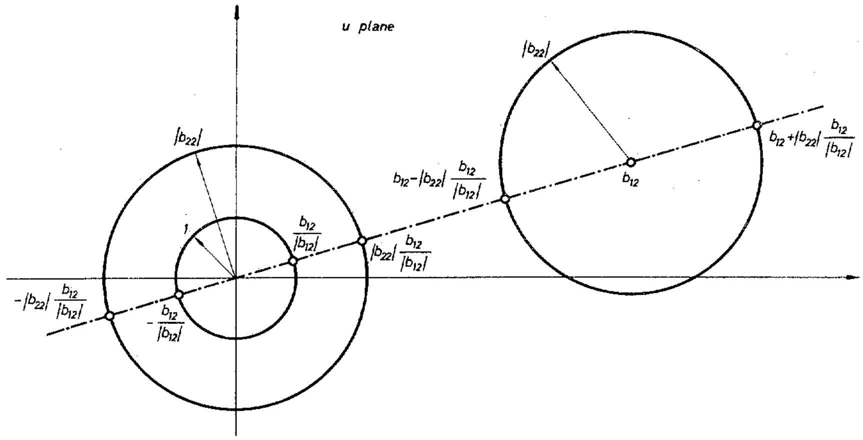


Fig. 13. Mapping the unit circle by the transformation $u = b_{12} + b_{22}z_1$.

where

$$\mu = -b_{21}/b_{22}$$

$$\nu = -b_{11} + (b_{21}/b_{22})b_{12}.$$

The transformation (B6) can be considered as a combination of the following transformations:

$$u = b_{12} + b_{22}z_1$$

$$v = 1/u$$

$$z_2 = \mu + \nu v$$

namely, the product of a similarity, an inversion, and another similarity.

The similarity has the property of mapping straight lines into straight lines and so does the inversion $v = 1/u$ for those straight lines crossing the origin in the $u$ plane. Since our domain of interest is $\{z_1: |z_1| = 1\}$, the points in the $u$ plane lying on a straight line crossing the origin, and that, according to the transformation $u = b_{12} + b_{22}z_1$, are images of some $z_1$ such that $|z_1| = 1$, are the following (see Fig. 13):

$$u_A = b_{12} - |b_{22}|(b_{12}/|b_{12}|) \tag{B7}$$

$$u_B = b_{12} + |b_{22}|(b_{12}/|b_{12}|). \tag{B8}$$

Therefore, by the transformation

$$z_2 = -b_{21}/b_{22} - [b_{11} - (b_{21}/b_{22})b_{12}](1/u)$$

the points $z_{2A}$ and $z_{2B}$ are

$$z_{2A} \triangleq z_2|_{u=u_A} = -\frac{b_{21}}{b_{22}} - \frac{b_{11}b_{22} - b_{21}b_{12}}{b_{22}} \frac{|b_{12}|}{b_{12}(|b_{12}| - |b_{22}|)} \tag{B9}$$

$$z_{2B} \triangleq z_2|_{u=u_B} = -\frac{b_{21}}{b_{22}} - \frac{b_{11}b_{22} - b_{21}b_{12}}{b_{22}} \frac{|b_{12}|}{b_{12}(|b_{12}| + |b_{22}|)}. \tag{B10}$$

Substituting (B9) and (B10) into (B4) and (B5) the center and the radius are

$$c = \frac{z_{2A} + z_{2B}}{2} = \frac{b_{21}b_{22}^* - b_{11}b_{12}^*}{|b_{12}|^2 - |b_{22}^2|}$$

$$r = \frac{z_{2A} - z_{2B}}{2} = \frac{b_{11}b_{22} - b_{21}b_{12}}{|b_{12}|^2 - |b_{22}|^2}. \qquad \text{Q.E.D.}$$

*Corollary*

If the coefficients $b_{11}$, $b_{21}$, $b_{12}$, and $b_{22}$ of (B1) are defined by (11) the center $c$ and the radius $r$ of the circle image are given by

$$c_i = -\frac{a_i}{a_i + \cos\beta} \tag{B11}$$

$$r_i = \frac{\cos\beta}{a_i + \cos\beta} \tag{B12}$$

where $a_i = \mathrm{Re}\,[(T/2)p_i]$.

*Remarks*

Note that the center given by (B11) indicates that it will always lie on the real axis. If $a_i + \cos\beta = 0$ the circle image becomes a straight line perpendicular to the real axis at the point $(-1,0)$.

## REFERENCES


[1] T. S. Huang, "Two-dimensional windows," *IEEE Trans. Audio Electroacoust.* (Corresp.), vol. AU-20, pp. 88–89, Mar. 1972.

[2] J. V. Hu and L. R. Rabiner, "Design techniques for two-dimensional digital filters," *IEEE Trans. Audio Electroacoust.* (*Special Issue on Digital Filtering*), vol. AU-20, pp. 249–257, Oct. 1972.

[3] J. H. McClellan, "The design of two-dimensional digital filters by transformations," in *Proc. Seventh Annu. Princeton Conf. on Information Sciences and Systems*, Mar. 1973, pp. 247–251.

[4] E. L. Hall, "A comparison of computations for spatial frequency filtering," *Proc. IEEE* (*Special Issue on Digital Picture Processing*), vol. 60, pp. 887–891, July 1972.

[5] C. H. Farmer and D. S. Gooden, "Rotation and stability of a recursive digital filter," in *Proc. Two-Dimensional Digital Signal Processing Conf.*, Columbia, Mo., Oct. 1971, pp. 1-2-1–1-2-12.

[6] J. L. Shanks, S. Treitel, and J. H. Justice, "Stability and synthesis of two-dimensional recursive filters," *IEEE Trans. Audio Electroacoust.*, vol. AU-20, pp. 115–128, June 1972.

[7] T. S. Huang, "Stability of two-dimensional recursive filters," *IEEE Trans. Audio Electroacoust.*, vol. AU-20, pp. 158–163, June 1972.

[8] J. M. Costa, "Design and realization of stable two-dimensional recursive filters," M.A.Sc. thesis, Univ. of Toronto, Toronto, Ont., Canada, Sept. 1973.

[9] G. A. Maria and M. M. Fahmy, "An $l_p$ design technique for two-dimensional digital recursive filters," *IEEE Trans. Acoust., Speech, Signal Processing*, vol. ASSP-22, pp. 15–21, Feb. 1974.

[10] R. M. Golden, "Digital filters synthesis by sampled-data transformation," *IEEE Trans. Audio Electroacoust.* (*Special Issue on Digital Filters: The Promise of LSI Applied to Signal Processing*), vol. AU-16, pp. 321–329, Sept. 1968.

[11] L. R. Rabiner and B. Gold, "Processing of two-dimensional signals," unpublished notes, May 1972.

[12] W. Rudin, *Real and Complex Analysis*. New York: McGraw-Hill, 1966, p. 270.

# Recursive Filter Design Using Differential Correction

DAN E. DUDGEON, MEMBER, IEEE

*Abstract*—**Recent work by Thajchayapong and Rayner [1] demonstrated a technque for designing recursive infinite impulse response (IIR) digital filters by linear programming. By using an algorithm, described by Barrodale *et al.* [2], the differential correction algorithm, we will show how one may obtain optimum rational approximations to a given magnitude-squared frequency response in the Chebyshev norm. This optimization may be carried out on disjoint sets of frequency points obviating specification of the given magnitude-squared frequency response in transition bands. In addition, it will be shown how the differential correction algorithm is easily generalized to include weighted Chebyshev approximation.**

## INTRODUCTION

THE DESIGN of infinite impulse response (IIR) digital filters is inherently a nonlinear, complex approximation problem. It can be made into a nonlinear real approximation problem by considering only the magnitude squared (or magnitude) of the frequency response of the filter and the ideal function which is being approximated. One approach has been to use nonlinear optimization techniques to minimize the error of the approximation [3], [4]. Another has been to restructure the problem so that linear programming (a linear optimization technique) may be used to minimize an error functional [1], [5].

In this paper, we will use the differential correction algorithm described by Barrodale *et al.* [2] to design recursive filters with optimum (in the Chebyshev, or minimax, sense) magnitude-squared frequency responses. In addition, we will show that the optimization may be carried out over disjoint frequency intervals, and that weighted Chebyshev approximation is possible with this algorithm.

Manuscript received January 4, 1974; revised February 26, 1974. This work was supported in part by the Advanced Research Projects Agency of the Department of Defense, monitored under Contract N0014-67-A-0204-0064 and the Massachusetts Institute of Technology Lincoln Laboratory (sponsored in part by the U.S. Air Force). This paper was based on work forming a part of a dissertation to be submitted to the Department of Electrical Engineering, Massachusetts Institute of Technology, Cambridge, in partial fulfillment of the requirements for the Doctor of Science degree.

The author is with Bolt, Beranek, and Newman, Inc., Cambridge, Mass. 02138.

For convenience, we will use the notation $H(\omega)$, rather than $H(e^{j\omega})$ to denote Fourier transforms.

Once a magnitude-squared function $R(\omega) = |H(\omega)|^2$ has been designed, it is possible to implement the designed frequency characteristics exactly with no phase distortion by the following scheme. If $x(n)$ is the input and $h(n)$ is the realizable unit sample response whose Fourier transform has the magnitude-squared function $R(\omega)$, then first filter $x(n)$ by $h(n)$ to get an output $c(n)$. Then filter $c(-n)$ by $h(n)$ to get an output $d(n)$. The sequence $y(n) = d(-n)$ will then have a transform

$$Y(\omega) = R(\omega)\, X(\omega).$$

At this point it should be noted that a similar technique can be applied by designing the real function $2\mathrm{Re}[G(\omega)]$ where Re denotes "the real part of." Again let $x(n)$ be the input. Let $g(n)$ be the realizable unit sample response whose transform has a real part equal to the designed $\mathrm{Re}[G(\omega)]$. First, filter $x(n)$ by $g(n)$ to get an output $p(n)$. Also, filter $x(-n)$ by $g(n)$ to get $s(n)$. Then the sequence $y(n) = p(n) + s(-n)$ will have the desired transform

$$Y(\omega) = 2\mathrm{Re}[G(\omega)]X(\omega).$$

This second technique may actually be preferable to the first since the two filtering operations are done in parallel, and since the function $2\mathrm{Re}[G(\omega)]$ is not constrained to be nonnegative whereas the function $R(\omega)$ must be nonnegative.

Of course, the minimum phase frequency response whose magnitude squared is $R(\omega)$ may be realized by factoring the denominator and numerator polynomials, keeping the poles and zeros inside the unit circle, and forming a cascade of second-order sections, for example.